

# Investigation of ionic conductivity of lanthanum cerium oxide nano crystalline powder synthesized by co precipitation method

Hozefa Tinwala <sup>a</sup>, Patij Shah <sup>a</sup>, Kirit Siddhapara <sup>a</sup>, Dimple Shah <sup>a,\*</sup>, Jyoti Menghani <sup>b</sup>

<sup>a</sup> Applied Physics Department, Sardar Vallabhbhai National Institute of Technology, Surat 395007, India

<sup>b</sup> Mechanical Engineering Department, Sardar Vallabhbhai National Institute of Technology, Surat 395007, India

## ARTICLE INFO

### Keywords:

- A1. Crystal morphology
- A2. Co-precipitation method
- B1. Lanthanum Cerium Oxide ( $\text{La}_2\text{Ce}_2\text{O}_7$ )
- B1. Nanomaterials
- B1. Oxides

## ABSTRACT

Lanthanum (La) doped Ceria ( $\text{CeO}_2$ ) electrolyte has attracted considerable interest, as a candidate material for solid oxide fuel cells (SOFCs). The ionic conductivity of La doped  $\text{CeO}_2$  system ( $\text{La}_2\text{Ce}_2\text{O}_7$ ) nano-particles synthesized by the co-precipitation method has been investigated. The cubic fluorite structure was observed from the structural analysis of the material. Morphology of the sintered pellets are observed by scanning electron microscope (SEM), respectively. From the results of impedance spectroscopy from temperature range of room temperature to 400 °C, the oxide ion conductivity due to proton charge carrier was observed. Thermogravimetric analysis (TGA) was performed on the material to check stability of phase at high temperature.

© 2016 Elsevier B.V. All rights reserved.

## 1. Introduction

Rare earth doped cerium oxide with fluorite structure [1,2] has attracted considerable attentions due to its excellent electrical properties [3]. Conductivity in oxides occurs due to the presence of oxygen vacancies created by replacing foreign cations with lower valency parent cations. For example oxygen vacancies in Lanthanum Cerium Oxide ( $\text{La}_2\text{Ce}_2\text{O}_7$ ) are created by replacing  $\text{Ce}^{4+}$  cations in Cerium Oxide ( $\text{CeO}_2$ ) with  $\text{La}^{3+}$  cations from Lanthanum Oxide ( $\text{La}_2\text{O}_3$ ) and systems in [4–9].

Oxides with fluorite structure such as rare earth doped ceria ( $\text{La}_2\text{Ce}_2\text{O}_7$ ) find applications in various fields such as oxygen sensor, oxygen pump, solid oxide fuel cells (SOFC) etc., due to their capacity to accept considerable amount of oxygen vacancy. The phase of crystal and oxide ion conductivities are considerably influenced by cation radius ratio and lattice constant [10].

In the present paper, structural properties, phase stability, and ionic conductivity of  $\text{La}_2\text{Ce}_2\text{O}_7$  has been studied.

## 2. Experimental procedure

The precursors used for the synthesis of Lanthanum Cerium Oxide ( $\text{La}_2\text{Ce}_2\text{O}_7$ ) nanoparticles were Lanthanum nitrate hexahydrate  $\text{La}(\text{NO}_3)_3 \cdot 6\text{H}_2\text{O}$  (Loba Chemie 99%) and Cerium nitrate hexahydrate

( $\text{Ce}(\text{NO}_3)_3 \cdot 6\text{H}_2\text{O}$ ). The precipitant and solvent used were triethylamine ( $\text{C}_2\text{H}_5)_3\text{N}$  and ethanol respectively. Precipitation was performed at room temperature. In a typical synthesis both the precursors are dissolved in 100 ml of absolute ethanol to make 0.1 M solutions, then both solutions were mixed in a single beaker and kept for stirring at room temperature for 1 h. After that 200 ml of 1.2 M triethylamine (TEA) was added to 200 ml ethanol in another beaker and then later solution was added in the previous solution drop by drop with constant speed of one drop per second. Initially the pH of the solution before adding mixture of triethylamine (TEA) and ethanol drop wise was 4.0. After the drop wise addition of triethylamine (TEA) and ethanol mixture, the pH started increasing, the formation of precipitates occurred at 8.9 pH. The stirring was continued for 1 h after the completion of precipitation, and the solution was filtered by a suction filter using Whatman 42 (pore diameter 2.5 μm) filter paper. The completion of precipitation was confirmed by adding 10 mL of filtrate with ammonium hydroxide solution. Before drying at room temperature for 24 h, the precipitate was washed with the solvent alcohol several times. The resulting powder was then washed with acetone to remove the remaining alcohol, unreacted triethylamine, and other by-products. The as-prepared material was then calcined at different temperature for 3 h. The process for making  $\text{La}_2\text{Ce}_2\text{O}_7$  was followed according to the work reported by Li et al. [11].

The synthesis of  $\text{La}_2\text{Ce}_2\text{O}_7$  by the co-precipitation method, goes under many chemical reactions: oxidation of  $\text{Ce}^{3+}$  to  $\text{Ce}^{4+}$  and hydration of  $\text{Ce}^{4+}$  and  $\text{La}^{3+}$  which is then followed by the formation of a  $[\text{Ce}(\text{H}_2\text{O})_x(\text{OH})_y]^{(4-y)+}$  and  $[\text{La}(\text{H}_2\text{O})_x(\text{OH})_y]^{(3-y)+}$  complex (color change from colorless to pinkish purple), deprotonation of the hydrated complex to form hydrated  $\text{La}_2\text{Ce}_2\text{O}_7$

\* Corresponding author. Tel.: +91 9714504517.

E-mail addresses: [t.hozefa@ashd.svnit.ac.in](mailto:t.hozefa@ashd.svnit.ac.in) (H. Tinwala), [dshah@ashd.svit.ac.in](mailto:dshah@ashd.svit.ac.in), [dimpleshah73@yahoo.co.in](mailto:dimpleshah73@yahoo.co.in) (D. Shah).

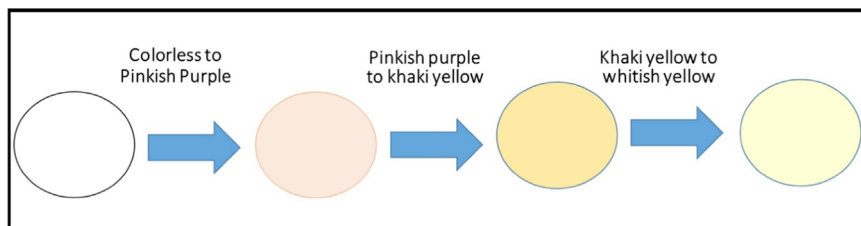
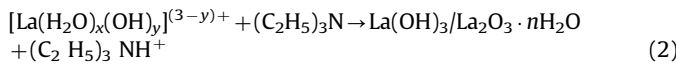
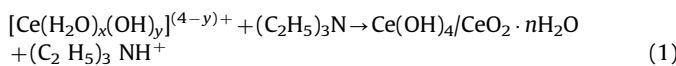


**Fig. 1.** Schematic diagram of color change during each step of process.

(color change from pinkish purple to khaki yellow), and finally dehydration of the hydrated  $\text{La}_2\text{Ce}_2\text{O}_7$  to form  $\text{La}_2\text{Ce}_2\text{O}_7$  powder (color change from khaki yellow to whitish yellow) (Fig. 1).

During the whole process of precipitation, the deprotonation process occurs very slowly, which also depends on the precipitating agent utilized. Again, due to the strong basicity and higher charge, Ce and La ions usually undergo strong hydration, giving rise to the formation of  $[\text{Ce}(\text{H}_2\text{O})_x(\text{OH})_y]^{(4-y)+}$  and  $[\text{La}(\text{H}_2\text{O})_x(\text{OH})_y]^{(3-y)+}$  complex, where  $(x+y)$  is the coordination number of  $\text{Ce}^{4+}$  and  $\text{La}^{3+}$ . The following reaction takes place



Thus,  $\text{Ce}(\text{OH})_4/\text{CeO}_2 \cdot n\text{H}_2\text{O}$  and  $\text{La}(\text{OH})_3/\text{La}_2\text{O}_3 \cdot n\text{H}_2\text{O}$  forms even at room temperature in the solution. Rapid deprotonation of  $[\text{Ce}(\text{H}_2\text{O})_x(\text{OH})_y]^{(4-y)+}$  and  $[\text{La}(\text{H}_2\text{O})_x(\text{OH})_y]^{(3-y)+}$  has a major effect on the morphology of the nanocrystalline  $\text{La}_2\text{Ce}_2\text{O}_7$  powders.

Other methods such as solid state method and cold pressing method, forms micron sized particles and requires more heating time. Water is used as solvent for the synthesis of  $\text{La}_2\text{Ce}_2\text{O}_7$  in case of the hydrothermal and conventional co-precipitation method. As water is used as solvent, there arises the possibility of hard agglomerate formation due to hydrogen bonds. In the method used by us, the only water used is molecular water in the precursors, thus hard agglomerates are not formed.

XRD (Bruker's D2 Phaser) and SEM were used to characterize phase and particle size, EDS was used to verify the stoichiometric composition,  $\text{La}_2\text{Ce}_2\text{O}_7$  powder, TG-DSC was used to study the stability of the  $\text{La}_2\text{Ce}_2\text{O}_7$  particles and Impedance spectroscopy was used to measure the contribution of proton in overall conductivity.

### 3. Results and discussion

#### 3.1. X-Ray diffraction analysis (XRD)

Fig. 2 shows the X-ray diffraction pattern of  $\text{La}_2\text{Ce}_2\text{O}_7$  sample calcined for 3 h at 800 °C.

X-ray diffraction study (XRD) analysis was performed using Bruker X-ray diffractometer (D2 Phaser). Cubic fluorite phase of  $\text{CeO}_2$  can be observed from the diffraction pattern of the XRD graph. Fluorite type structure can accept considerable amount of oxygen vacancies. Crystallite size calculated by Scherrer's equation is 16 nm for sample calcined at 800 °C.

Also, individual oxides ( $\text{La}_2\text{O}_3$  etc.) are not observed in the XRD pattern.

#### 3.2. Scanning electron microscopy (SEM)

Fig. 3 shows the SEM image of  $\text{La}_2\text{Ce}_2\text{O}_7$  tablet of nanopowder calcined at 800 °C. Hitachi S3400N and Geon 5610 model with Oxford Olympus software were utilized for measurement. From the figure it

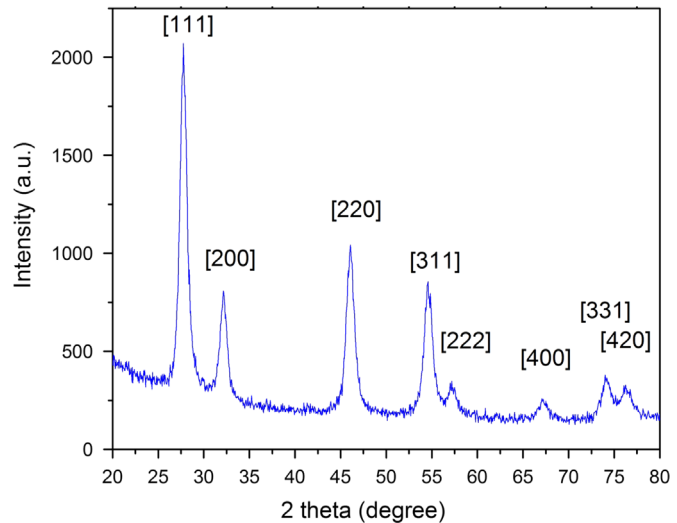


**Fig. 2.** XRD pattern of  $\text{La}_2\text{Ce}_2\text{O}_7$  nanoparticles.



**Fig. 3.** SEM micrograph of  $\text{La}_2\text{Ce}_2\text{O}_7$  powder tablet.

can be observed that the sample is dense with no segregation of secondary phase in XRD measurement.

#### 3.3. Energy dispersive spectroscopic (EDS) analysis

EDS measurements were done for  $\text{La}_2\text{Ce}_2\text{O}_7$  nanopowder calcined at 800 °C for 3 h, as shown in Fig. 4. The chemical composition of the sample measured in atomic percentage is approximately equal to the stoichiometric composition of  $\text{La}_2\text{Ce}_2\text{O}_7$ .

There are 64.30% oxygen, 17.82% lanthanum and 17.88% cerium atoms present in the material, as observed by EDS measurements, which is almost equal to the metal amount taken during synthesis.

#### 3.4. Thermogravimetric analysis (TGA) and differential scanning calorimetry (DSC)

Fig. 5 shows the TG and DSC curves for  $\text{La}_2\text{Ce}_2\text{O}_7$  powder. Thermogravimetric analysis (TGA) was studied from room

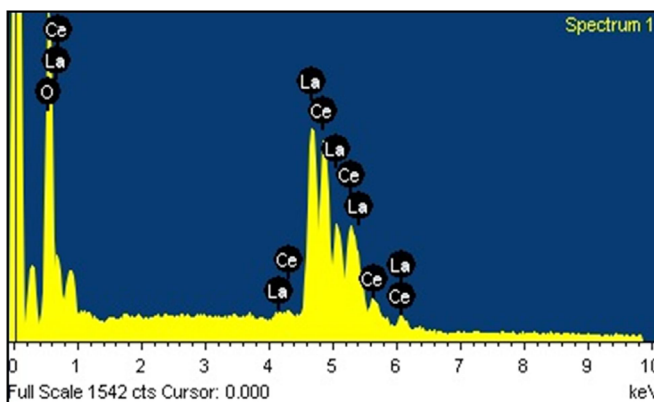


**Fig. 4.** EDS of  $\text{La}_2\text{Ce}_2\text{O}_7$  powder.

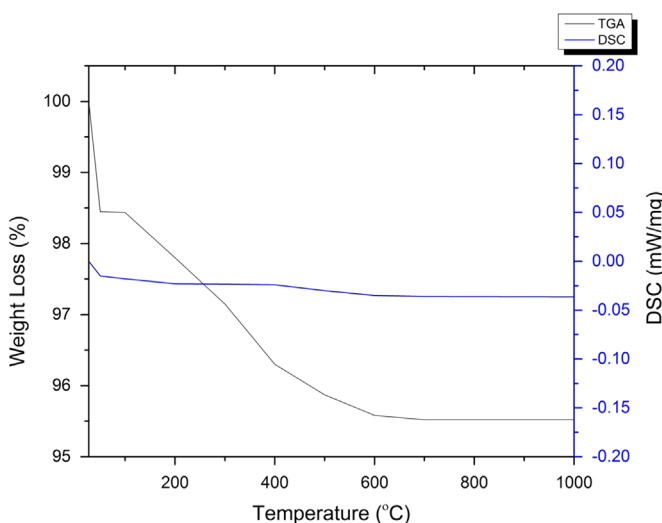


**Fig. 5.** TG and DSC analysis of  $\text{La}_2\text{Ce}_2\text{O}_7$  powder.

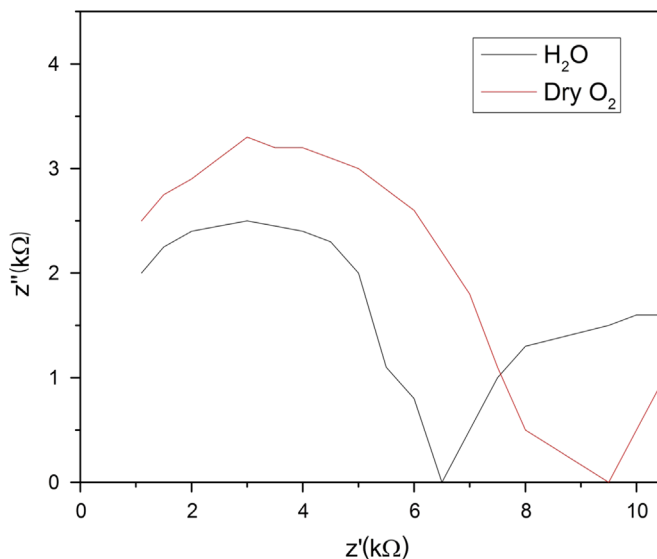


**Fig. 6.** Impedance spectra of  $\text{La}_2\text{Ce}_2\text{O}_7$  at 400 °C under wet and dry  $\text{O}_2$ .

temperature to 1000 °C at a heating rate of 10 °C/min under nitrogen atmosphere having a flow rate of 20 mL/min. The weight loss occurs in two stages, first stage taking place from room temperature up to 100 °C, the weight loss during first stage occurs due to the evaporation of moisture. The weight loss during second

stage from temperature 150 °C up to 600 °C occurs due to residual organic substances and decomposition of organic groups formed during synthesis.

There is neither endothermal nor exothermal peaks in the DSC curve shown in Fig. 4 implying that  $\text{La}_2\text{Ce}_2\text{O}_7$  has high phase stability from room temperature up to 1000 °C.

### 3.5. Impedance spectroscopy

Fig. 6 shows Nyquist representation of impedance spectra. From the above figure it can be observed that there is negligible contribution from grain boundary impedance in the spectra. Also, the influence of proton in overall conductivity can be observed clearly from the figure.

## 4. Conclusion

$\text{La}_2\text{Ce}_2\text{O}_7$  nanoparticles have been synthesized via co-precipitation method, which is simple and cost effective.

1. From XRD pattern of  $\text{La}_2\text{Ce}_2\text{O}_7$  calcined at 800 °C, phase stability at higher temperature was observed as there is no phase change.
2. From SEM analysis no segregation of secondary phase is observed, and EDS measurements verified the stoichiometric composition of  $\text{La}_2\text{Ce}_2\text{O}_7$ .
3. Impedance spectra shows the contribution of proton in overall conductivity.

## References

- [1] F. Ye, T. Mori, D.R. Ou, J. Zou, J. Drennan, A structure model of nano-sized domain in Gd-doped ceria, Solid State Ion. 180 (2009) 1414–1420.
- [2] M. Godinho, R. Gonçalves, L.S. Santos, J.A. Varela, E. Longo, E. Leite, Room temperature co-precipitation of nanocrystalline  $\text{CeO}_2$  and  $\text{Ce}_{0.8}\text{Gd}_{0.2}\text{O}_{1.9-\delta}$  powder, Mater. Lett. 61 (2007) 1904–1907.
- [3] H. Tuller, A. Nowick, Doped ceria as a solid oxide electrolyte, J. Electrochem. Soc. 122 (1975) 255–259.
- [4] J. Goodenough, J. Ruiz-Diaz, Y. Zhen, Oxide-ion conduction in  $\text{Ba}_2\text{In}_2\text{O}_5$  and  $\text{Ba}_3\text{In}_2\text{Mo}_8$  ( $M=\text{Ce}, \text{Hf}, \text{or Zr}$ ), Solid State Ion. 44 (1990) 21–31.
- [5] T. Norby, Fast oxygen ion conductors – from doped to ordered systems Basis of a presentation given at Materials Discussion no. 3, 26–29 September, 2000, University of Cambridge, UK, J. Mater. Chem. 11 (2001) 11–18.
- [6] R. Strandbakke, C. Kongshaug, R. Haugsrud, T. Norby, High-temperature hydration and conductivity of mayenite,  $\text{Ca}_{12}\text{Al}_{14}\text{O}_{33}$ , J. Phys. Chem. C 113 (2009) 8938–8944.
- [7] M. Verkerk, K. Keizer, A. Burggraaf, High oxygen ion conduction in sintered oxides of the  $\text{Bi}_2\text{O}_3$ – $\text{Er}_2\text{O}_3$  system, J. Appl. Electrochem. 10 (1980) 81–90.
- [8] T. Takahashi, H. Iwahara, T. Arao, High oxide ion conduction in sintered oxides of the system  $\text{Bi}_2\text{O}_3$ – $\text{Y}_2\text{O}_3$ , J. Appl. Electrochem. 5 (1975) 187–195.
- [9] S. Noirault, S. Celierier, O. Joubert, M.T. Caldes, Y. Piffard, Effects of water uptake on the inherently oxygen-deficient compounds  $\text{Ln}_{26}\text{O}_{27}(\text{BO}_3)_8$  ( $\text{Ln}=\text{La, Nd}$ ), Inorg. Chem. 46 (2007) 9961–9967.
- [10] H. Yamamura, H. Nishino, K. Kakimoto, Ac conductivity for  $\text{Eu}_2\text{Zr}_2\text{O}_7$  and  $\text{La}_2\text{Ce}_2\text{O}_7$  with pyrochlore-type composition, J. Ceram. Soc. Jpn. 112 (2004) 553–558.
- [11] J.G. Li, T. Ikegami, J.H. Lee, T. Mori, Characterization and sintering of nanocrystalline  $\text{CeO}_2$  powders synthesized by a mimic alkoxide method, Acta Mater. 49 (2001) 419–426.